Transfer and backtransfer processes in Yb^{3+}–Er^{3+} codoped Strontium Barium Niobate glass-ceramics

L.L. Martín*, I.R. Martín [1], P. Haro-González

Departamento de Física Fundamental y Experimental, Electrónica y Sistemas, Universidad de La Laguna 38206 La Laguna, S/C de Tenerife, Spain

ABSTRACT

The forward and backward energy transfer processes in Strontium Barium Niobate glass-ceramics double doped with Yb^{3+} and Er^{3+} ions have been studied. In these samples the rare earth ions are incorporated into the nanocrystals with an average size of 50 nm. Using laser excitation at 950 nm is possible to excite selectively the Yb^{3+} ions and detect emission due to these ions (at 1040 nm) or combined with the Er^{3+} ions (at 980 nm). In previous works, the energy transfer processes between these ions in different matrices have been analyzed in order to improve the emission at 1550 nm, but these analyses are restricted to fast migration processes among ions. In this fast migration regimen the results are valid only for larger concentrations. However, in this work the dynamics of these transfer processes has been carried out using a general method called "transfer function model". The parameters which characterize these processes have been obtained and it has been possible to explain the important increase of the emission at 1550 nm due to the co-doping with Yb^{3+} ions. This analysis is valid for any range of doping concentrations.

© 2011 Elsevier B.V. All rights reserved.

1. Introduction

Strontium Barium Niobate (SBN) is a fascinating family of ferroelectric mixed crystals with a great number of potential applications in photonics, such as optical data storage, switching and optical computing, due to its excellent electro-optics, acusto-optics, piezoelectric and non-linear coefficients [1–4]. During its growth, it can be easily doped with rare earth and transition metal ions, improving its potential technological application. Doping with Ce^{3+} or Cr^{3+} has been demonstrated to increase its photorefractive properties [5], and with Nd^{3+} ions leads to self-frequency converted diode-pumped tunable lasers emitting coherent radiation in the near infrared and simultaneously in visible regions of the spectra [6]. However, the growth of the SBN crystals is normally expensive and difficult [7]. Therefore, alternative methods to obtain this matrix are interesting for the scientific community.

In a recent work, our research group presented SBN glass ceramic samples obtained from a thermal treatment of precursor glass in a simple and "industrialization suitable" method. The SBN glass ceramics were doped with Er^{3+} ions and produced an enhancement of the up-conversion luminescence at 800 nm excitation, due to the incorporation of these ions into the SBN nanocrystals [8].

In order to extend the knowledge and the application perspective of this material, it has been studied the optical properties under excitation at 975 nm in Er^{3+} single doped samples and in Er^{3+}–Yb^{3+} codoped samples. Er^{3+} ions have a relatively low absorption cross-section for the transitions in the near-infrared (NIR) region around 1000 nm. On the other hand, Yb^{3+} ions exhibit a much larger absorption cross-section in this region and thus, co-doping with Yb^{3+} ions has demonstrated to be a successful alternative for the up-conversion process [9,10] or to increase the emission at 1550 nm coming from Er^{3+} ions [11].

In fact, there is a large spectral overlap between the $^2F_{5/2} \rightarrow {}^2F_{7/2}$ (Yb^{3+}) transition and the $^4I_{15/2} \rightarrow {}^4I_{11/2}$ (Er^{3+}) absorption bands, which results in an efficient energy transfer. The efficiency of this process is limited by the back energy transfer from the various excited levels of the Er^{3+} to Yb^{3+} ions. The dynamic of these forward and backward processes needs to be well understood in order to optimize the efficiency of the up-conversion systems or the emission at 1550 nm.

This work, presents the dynamics of the transfer and back-transfer process among Yb^{3+} ($^2F_{5/2}$) and Er^{3+} ($^4I_{11/2}$) ions in codoped SBN glass ceramic samples, after selective excitation of each ion. This dynamics has been analyzed using the fluorescence "transfer function model" [12,13] and in this sense has been

* Correspondence to: Departamento de Física Fundamental y Experimental, Electrónica y Sistemas, Facultad de Fisica, Av. Astrofisico Francisco Sanchez s/n, Universidad de La Laguna E-38206 La Laguna, S/C de Tenerife, Spain. Tel.: +34922318651.

E-mail address: lmartin@ull.es (L.L. Martín).
[1] MALTA Consolider Team.

possible to explain the increase of the emission at 1550 nm and to simulate its dependence with the concentration of Er^{3+} or Yb^{3+} ions.

2. Experimental

The precursor glasses were fabricated by the standard melt quenching method with the following composition: RE_2O_3–SrO–BaO–Nb_2O_5–B_2O_3 (where RE=Er^{3+} or Yb^{3+}). The glass ceramic samples were obtained by thermal treatment of this precursor glass at 620 °C for 2 h and were formed by glassy and crystalline phase of SBN nanocrystals with a medium size of 50 nm [8].

Absorption spectra were measured by a Perkin-Elmer 9 UV–vis–NIR spectrophotometer. The optical excitation of the glass ceramic samples were developed by an optical parametric oscillator (OPO) tuned to requested wavelengths with 5 ns pulses and by continuous wave diode lasers at 800 and 950 nm. The detection equipment was a TRIAX-180 monochromator with 0.5 or 1 nm resolution in the VIS or the NIR range, respectively. An extended PMT or an InGaAs detector was used at the output of the monochromator to detect the emission. For time resolved experiments the signal was registered by a digital oscilloscope TEK-TRONIX-2430A. All experiments were carried out at room temperature.

3. Theoretical review

When the interaction between luminescent ions is not important, the decay of the luminescence can be fitted to a single exponential. However when ion concentration is large enough, energy transfer could appear and the decay curves become non-exponential. If we consider interaction between donors (initially excited ions) and acceptors (traps for the energy), then the expression derived by Inokuti and Hirayama [14] can describe the decay curves, i.e.

$$K_D(t) = I(0) \exp\left[-\frac{t}{\tau_D} - \frac{4\pi}{3}C_A\Gamma\left(1-\frac{3}{S}\right)(C_{DA}^{(S)}\,t)^{3/S}\right] \quad (1)$$

where τ_D is the intrinsic lifetime of the luminescent ions, $S=6$, 8 or 10 depending on the interaction character (dipole–dipole, dipole–quadrupole or quadrupole–quadrupole), C_A is the acceptor concentration, Γ Euler's gamma function and $C_{DA}^{(S)}$ is the donor–acceptor energy transfer parameter.

If we also consider energy transfer among donors (energy migration), the following generalized expression of the Yokota and Tanimoto model [15] could be used:

$$K_D(t) = I(0)\exp\left[-\frac{t}{\tau_D} - \frac{4\pi}{3}C_A\Gamma\left(1-\frac{3}{S}\right)(C_{DA}^{(S)}\,t)^{3/S}\left(\frac{1+a_1X+a_2X^2}{1+b_1X}\right)^{S-3/S-2}\right] \quad (2)$$

where the coefficients a_1, a_2 and b_1 are given in Table 1 and

$$X = D[C_{DA}^{(S)}]^{-2/S}\,t^{1-2/S} \quad (3)$$

Table 1
Coefficients a_1, a_2 and b_1 of Eq. (2).

S	Coefficients		
	a_1	a_2	b_1
6	10.866	15.500	8.743
8	17.072	35.860	13.882
10	24.524	67.909	20.290

where D is the diffusion parameter which characterizes the transfer between the donors.

Moreover, if the backtransfer processes from the acceptor to the donors under flash excitation are considered, the "transfer function" model could be used to study the kinetics of the forward and backward energy processes [12,13]. Therefore, the fluorescence for donors $I(t)$ and acceptors $G(t)$ could be expressed by

$$I(t) = L^{-1}\left[\hat{K}_D[(s+\tau_D^{-1})\hat{K}_D + (s+\tau_A^{-1})\hat{K}_A - (s+\tau_D^{-1})(s+\tau_A^{-1})\hat{K}_D\hat{K}_A]^{-1}\right]$$
(4)

$$G(t) = L^{-1}\left[\hat{I}(t)[\hat{K}_D^{-1} - (s+\tau_D^{-1})]\hat{K}_A\right] \quad (5)$$

where $\hat{f}$ and L^{-1} are the direct and inverse Laplace transform of $f(t)$ and τ_D and τ_A are the intrinsic lifetimes of donor and acceptor ions, respectively. Functions $K_D(t)$ and $K_A(t)$ indicate the dynamics of donors and acceptors (in single doped samples) under flash excitation. Therefore, $K_D(t)$ can be expressed by Eq. (1) or (2) and in similar way for $K_A(t)$.

4. Experimental results and discussion

4.1. Single doped samples

Generally, Er^{3+} ions have a low absorption coefficient at 975 nm corresponding to the $^4I_{15/2} \rightarrow {}^4I_{11/2}$ transition. For this reason, Er^{3+} doped matrix are usually codoped with Yb^{3+} ions in order to improve the absorption at this wavelength. As can be seen in Fig. 1, Yb^{3+}: $^2F_{7/2} \rightarrow {}^2F_{5/2}$ transition overlaps with Er^{3+}: $^4I_{15/2} \rightarrow {}^4I_{11/2}$ transition. The absorption is about five times larger in Yb^{3+} than in Er^{3+} samples with similar dopant concentrations.

Eq. (2) has been used to analyze the luminescence decays obtained in single doped samples with Er^{3+} or Yb^{3+} ions. As can be seen in Fig. 2 the decay curve of Yb^{3+} ions from the $^2F_{5/2}$ level can be fitted to a single exponential. However, the decay of Er^{3+} ions from the $^4I_{11/2}$ level fits well to Eq. (2) assuming $S=6$ (dipole–dipole) and negligible diffusion coefficient D among these ions. In this situation the dynamics for the Er^{3+} ions is well described by the following equation:

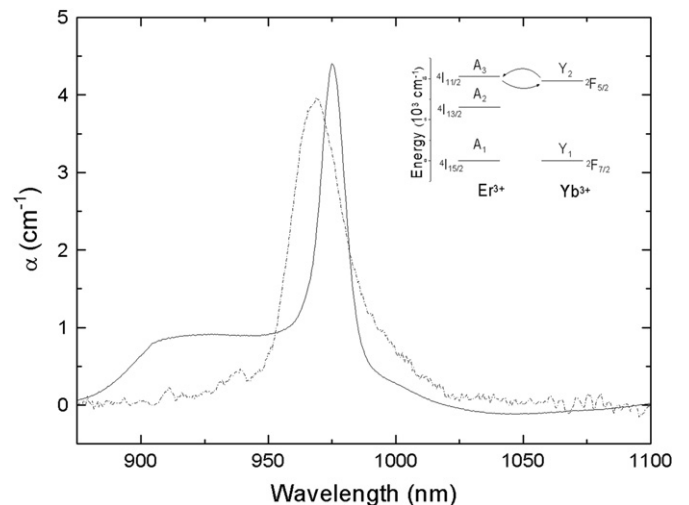$$K_A(t) = I_A(0)\exp\left[-\frac{t}{\tau_A} - \frac{4\pi}{3}C_A\sqrt{\pi}(C_{CREr}t)^{1/2}\right] \quad (6)$$

Fig. 1. Absorption spectra obtained in a glass ceramics sample single doped with 2.5 mol% of Er^{3+} (dashed line) and in a sample single doped with 1 mol% of Yb^{3+} (solid line). The inset shows the energy level diagram of Er^{3+} and Yb^{3+} ions.

where the C_A is the concentration of Er^{3+} ions and C_{CREr} is the cross relaxation parameter for the Er^{3+} ions and its value obtained from the fit is included in Table 2. These results indicate that the Er^{3+} ions in single doped samples have an important probability of cross relaxation process probably due to the following transfer channel

$$^4I_{11/2}, \, ^4I_{15/2} \rightarrow \, ^4I_{13/2}, \, ^4I_{13/2}$$
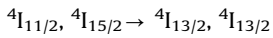
This energy transfer process is no resonant and therefore matrix phonons should be involved in the process.

4.2. Energy transfer processes in codoped samples

The Yb^{3+} and Er^{3+} ions in SBN have two resonant levels at about 975 nm as it is shown in the inset of Fig. 1. Therefore, when codoped samples are excited at 800 nm the effects of transfer processes can be observed. At this excitation wavelength, the Er^{3+} ions are excited to the $^4I_{9/2}$ level and immediately relax by multiphonon de-excitation to the $^4I_{11/2}$ level. In single Er^{3+} samples, the emission from this level to the ground state can be observed at 975 nm (see Fig. 3). However, in codoped samples, additional shoulders appear in this emission due to the $^2F_{5/2} \rightarrow \, ^2F_{7/2}$ transition at 975 nm coming from Yb^{3+} ions (see Fig. 3). This result indicates that the transfer processes from Er^{3+}:$^4I_{9/2}$ to Yb^{3+}:$^2F_{5/2}$ levels are appreciable.

Respect to the emission at 1550 nm coming from the Er^{3+} ions, as was mentioned in the introduction, codoped samples with Er^{3+} and Yb^{3+} ions could improve this emission when they are excited around 975 nm. This result can be seen in Fig. 4, where a spectacular increa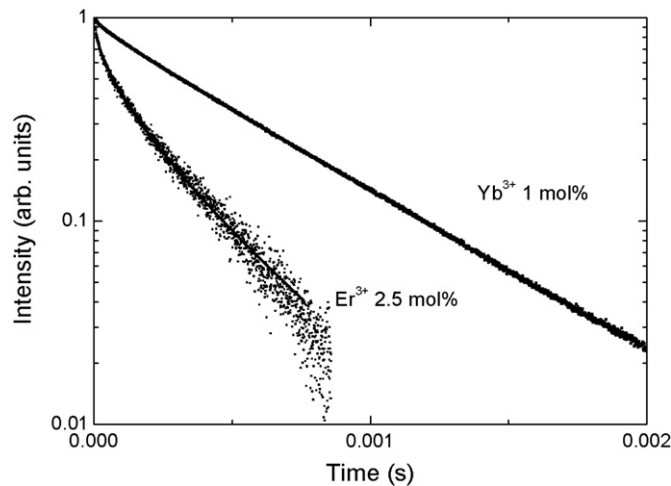se of the emission at 1550 nm is obtained in the codoped samples respect to the single Er^{3+} doped sample. This is explained due to the increase of the absorption at the excitation wavelength associated to the Yb^{3+} ions (see Fig. 1).

The result shown in Fig. 4 depends of the respective absorption of the ions at the excitation wavelength and the transfer and backtransfer processes between the Er^{3+} and Yb^{3+} ions. The knowledge of these processes is fundamental in order to improve
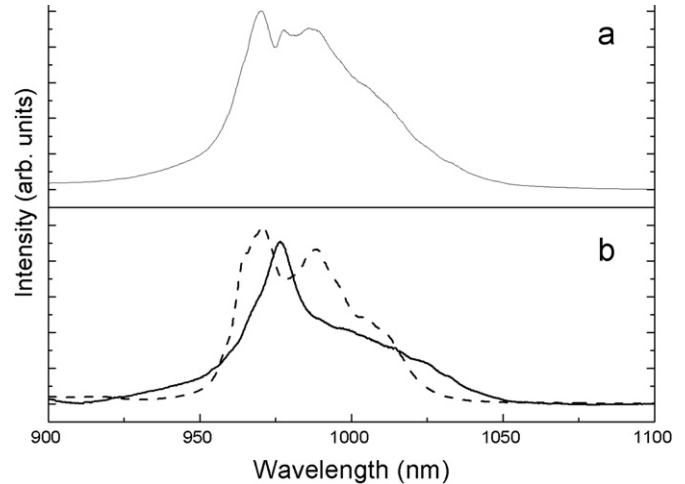
Fig. 3. Emission spectra obtained under excitation at 800 nm in (a) 2.5 mol% Er^{3+}–1 mol% Yb^{3+} codoped sample and (b) 2.5 mol% Er^{3+} single doped sample (dashed line) and 1 mol% Yb^{3+} single doped sample (solid line).
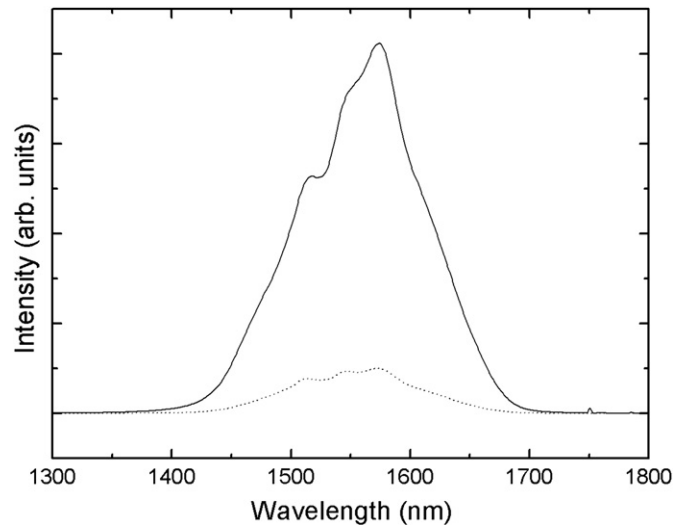
Fig. 2. Decay curves obtained from the $^2F_{5/2}$ level of Yb^{3+} ions and $^4I_{11/2}$ level of Er^{3+} ions in single doped samples. The solid lines correspond to the fits indicated in the text.

Fig. 4. Emission spectra obtained in a 2.5 mol% Er^{3+} single doped sample (dashed line) and in a 2.5 mol% Er^{3+}–1 mol% Yb^{3+} codoped sample (solid line) under excitation at 950 nm with a diode laser.

Table 2
Parameters used in the fits for a glass ceramics sample codoped with 2.5 mol% of Er^{3+} and 1 mol% of Yb^{3+}.

Er^{3+}						
C_A (at/cm^3)	σ_A (cm^2)	τ_A ($^4I_{11/2}$) (ms)	τ_2 ($^4I_{13/2}$) (ms)	C_{CREr} (cm^6 s^{-1})	W_{32} (s^{-1})	C_{AD} (cm^6 s^{-1})
9.0×10^{20}	8.84×10^{-23}	0.62	1.84	1.19×10^{-39}	1507	$< 0.01 \times 10^{-38}$

Yb^{3+}			
C_D (at/cm^3)	σ_D (cm^2)	τ_D ($^2F_{5/2}$) (ms)	C_{DA} (cm^6 s^{-1})
3.6×10^{20}	2.48×10^{-21}	0.51	3.6×10^{-38}

optical amplifiers in the 1550 nm region. Therefore, measurements of luminescence decays were carried out in codoped samples in order to analyze the dynamics of transfer and backtransfer processes. The dynamics of Yb^{3+} ions (considered as donors) could be described by Eq. (2) where the C_{DA} is the energy transfer parameter from Yb^{3+} ions (donors) to Er^{3+} ions (acceptors).

Respect to the dynamics of Er^{3+} ions, Eq. (6) obtained from Er^{3+} single doped samples has been generalized in order to take into account the $Er^{3+} \rightarrow Yb^{3+}$ transfer processes. In the previous fits obtained with this equation, it was shown that the diffusion processes among Er^{3+} ions into the level $^4I_{11/2}$ are negligible and the predominant interaction is dipole–dipole. Therefore, the dynamics for these ions in the codoped samples could be described by Eq. (2) for the donors and Eq. (7) for the acceptors

$$K_A(t) = I_A(0)\exp\left[-\frac{t}{\tau_A} - \frac{4\pi}{3}(C_A\sqrt{\pi}(C_{CREr}t)^{1/2} + C_D\sqrt{\pi}(C_{AD}\,t)^{1/2})\right] \quad (7)$$

where the C_{AD} is the energy transfer parameter from Er^{3+} ions (acceptor) to Yb^{3+} ions (donor).

Codoped samples have been excited at 950 nm in order to excite only the Yb^{3+} ions. As can be seen in Fig. 1, at 950 nm the absorption coefficient is negligible for Er^{3+} ions respect to Yb^{3+} ions. Therefore, temporal decay curves have been obtained exciting at this wavelength and detecting not in the same wavelengths. When the emission is obtained at 1040 nm, the emission of Er^{3+} is negligible (see Fig. 3), and the experimental decay curve is shown in Fig. 5. This decay is perfectly fitted by Eq. (4) and using Eqs. (2) and (7). The values for C_{DA} and C_{AD} given in Table 2 were obtained from these fits. As it is shown, the value for the backtransfer parameter is negligible indicating that when the Yb^{3+} ions are excited, there is an efficient transfer to Er^{3+} ions due to the high value of the C_{DA} parameter but the backtransfer process is not important. This result is very important because indicates that the Yb^{3+} ions can be used to excite efficiently the Er^{3+} ions.

When the decay curves are obtained exciting at 950 nm and detecting at 976 nm, some Er^{3+} emission contribution is expected at this wavelength. However, as can be seen in Fig. 5 both curves are very similar, indicating that the contribution to the emission of Er^{3+} ions at 976 nm is nearly negligible. This result indicates
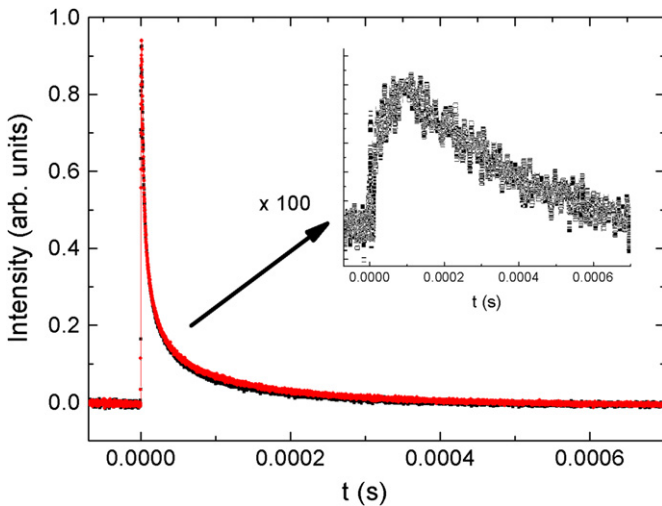

Fig. 5. Decay curves obtained in a 2.5 mol% Er^{3+}–1 mol% Yb^{3+} codoped sample exciting at 950 nm and detecting at 976 nm (red line) or 1040 nm (black line). The inset shows the difference of the decay curves multiplied by a factor 100. (For interpretation of the references to color in this figure legend, the reader is referred to the web version of this article.)

that there is a negligible backtransfer process from Er^{3+} to Yb^{3+} ions when the Yb^{3+} ions are excited directly.

5. Improving the emission at 1.5 μm

In order to explain the important increase observed in Fig. 4, the following model based in rate equations for this process have been proposed:

$$\frac{dA_3}{dt} = \sigma_A\varphi\,C_A - \left[\frac{1}{\tau_A} + W_{CREr}\right]A_3 + W_T Y_2 \quad (8)$$

$$\frac{dY_2}{dt} = \sigma_D\varphi\,C_D - \left[\frac{1}{\tau_D} + W_T\right]Y_2 \quad (9)$$

$$\frac{dA_2}{dt} = -\left[\frac{1}{\tau_2}\right]A_2 + [W_{32} + 2\,W_{CREr}]A_3 \quad (10)$$

In these equations, the populations of the Er^{3+} and Yb^{3+} levels are denoted as follows: Er^{3+}:$^4I_{13/2}$ is A_2, Er^{3+}:$^4I_{11/2}$ is A_3 and Yb^{3+}:$^2F_{5/2}$ is Y_2 as indicated in the inset of Fig. 1. The absorption cross sections of Er^{3+} ions and Yb^{3+} ions are σ_A and σ_D, respectively, and the incident pumping flux is φ. The terms τ_2 and τ_A indicate, respectively, the lifetimes of the A_2 and A_3 levels and the term τ_D is the lifetime of Y_2. W_{32} is the spontaneous emission probability between A_3 and A_2. The W_T parameter corresponds to the probability for the $Yb^{3+} \rightarrow Er^{3+}$ transfer process and the W_{CREr} parameter is the probability for the cross relaxation processes between Er^{3+} ions. In these equations have been neglected the backtransfer processes from Er^{3+} to Yb^{3+} ions according to the results obtained in the previous section.

In other works the analysis of the populations of the Er^{3+}–Yb^{3+} system has been made in similar way to our work but using constant values for the energy transfer parameters obtained from the decays curves [16]. These values are valid only when the rapid migration regimen has been reached and they are considered independent of the concentration. However, in the rates Eqs. (8–10) the transfer probabilities can be calculated as function of the concentration using the energy transfer parameters obtained in the previous section and presented in Table 1. Therefore, the transfer probability W_T can be calculated from Ref. [14]

$$W_T = \frac{\eta_T}{\tau_D(1-\eta_T)} \quad (11)$$

where η_T is the transfer efficiency and, as was previously mentioned, this energy transfer $Yb^{3+} \rightarrow Er^{3+}$ has a dipole–dipole character. Therefore, it could be obtained by Ref. [14]

$$\eta_T = \sqrt{\pi}\,x\,\exp(x^2)[1 - erf(x)] \quad (12)$$

where $erf(x)$ is the error function and x is given by

$$x = \frac{2\pi}{3}\sqrt{\pi}\,C_A\,C_{DA}^{1/2}\tau_D^{1/2} \quad (13)$$

where C_{DA} is the donor–acceptor energy transfer obtained from the fits to the temporal decay curves and it is given in Table 2. In similar way to these previous calculations the value for the W_{CREr} could be obtained using the values given in Table 2.

Under stationary regimen these equations can be solved and the population for the A_2 level is given by

$$A_2 = \tau_2\varphi\frac{W_{32}+2W_{CREr}}{(1/\tau_A)+W_{CREr}}\left[\sigma_A C_A + \sigma_D C_D\frac{W_T}{(1/\tau_D)+W_T}\right] \quad (14)$$

Therefore, it is possible to estimate the dependence of the intensity of the emission at 1550 nm (proportional to the population A_2) with the concentration of Er^{3+}. Fig. 6 shows the calculated dependences obtained in Er^{3+} single doped sample and in a Yb^{3+}–Er^{3+} codoped sample. As can be seen, for a
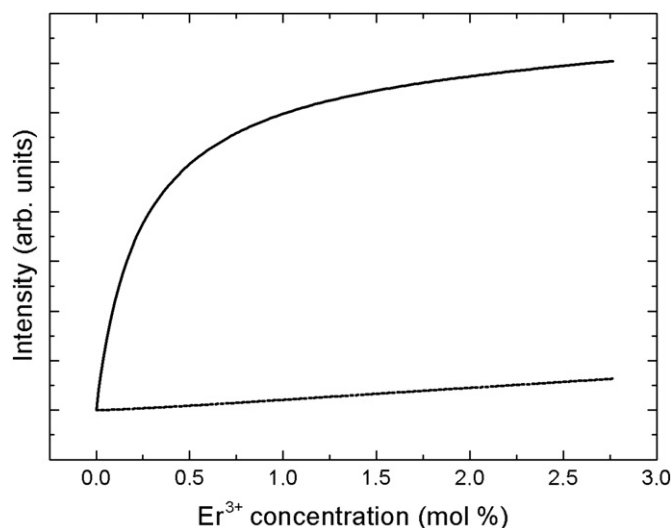
Fig. 6. Calculated emission intensity at 1.5 μm emission as function of Er^{3+} concentration for single doped glass ceramic sample (dashed line) and codoped sample with Er^{3+} and 1 mol% of Yb^{3+}.

concentration of 2.5 mol% of Er^{3+} it is estimated an increase about a factor 12 for the intensity when the sample is codoped with Yb^{3+} ions. This estimation is in good agreement with the results shown in Fig. 4. Moreover, this model could be used in order to explain similar experimental results obtained in different matrix codoped with Er^{3+}–Yb^{3+} ions [17,18]. As was previously mentioned, other works analyze the population of the $^4I_{13/2}$ using rate equations based in constant rates [16,19]. However, this treatment is valid only for the fast migration regimen between ions and only is valid for concentration larger than 4 or 5 mol% with Yb^{3+} ions. As example, in fluoroindate glasses doped with Yb^{3+} ions the transfer processes have been analyzed as function of the concentration, and for the maximum concentration of 2.25 mol% of Yb^{3+} has not been reached the fast migration regimen [20]. However, for laser or amplification experiments the optimum concentration usually is about 1 mol% and for this low doping concentration the fast migration regimen has not been reached among the optically active ions. Therefore, the treatment that the authors have carried out in this work let to analyze the population dynamics for any range of ion concentration.

6. Conclusions

In this work a general treatment has been used in order to analyze the transfer processes between the Er^{3+} and Yb^{3+} ions and the emission at 1.5 μm coming from Er^{3+} ions. The experimental results have been obtained with Yb^{3+}–Er^{3+} ions, which reside into SBN nanocrystals in a glass ceramics sample. The processes of forward and backward energy transfer processes have been analyzed using the "transfer function model" for the codoped samples and using the generalized Yokota–Tanimoto model for the dynamics of single doped samples. When the Yb^{3+} ions are directly excited there is an efficient transfer to Er^{3+} ions due to the high value of the energy transfer donor–acceptor parameter but the backtransfer process is negligible. The simulation of the population levels could be obtained for any range of concentrations and it is not limited to the fast migration regimen. Therefore, the results can explain the experimental increase of the intensity dependence for the emission at 1.5 μm when the sample is codoped with Yb^{3+} ions.

References

[1] P.V. Lenzo, E.G. Spencer, A.A. Ballman, Appl. Phys. Lett. 11 (1967) 23.
[2] R.R. Neurgaonkar, W.K. Cory, J. Opt. Soc. Am. B 3 (1986) 274.
[3] T. Granzow, Th. Woike, M. Wöhlecke, M. Imlau, W. Kleemann, Phys. Rev. Lett. 89 (2002) 127601.
[4] M. Goulkov, M. Imlau, T. Granzow, Th. Woike, J. Appl. Phys. 94 (2003) 4763.
[5] T.R. Volk, V. Yu., L.I. Salobutin, N.M. Ivleva, R. Polozkov, Pankrath, M. Woehlecke, Phys. Status Solidi 42 (2000) 2129.
[6] M.O Ramírez, J.J. Romero, P. Molina, L.E. Bausá, Appl. Phys. B 81 (2005) 827.
[7] G.A. Rakuljio, A. Yarw, R.R. Neurgaonkar, Opt. Eng. 25 (1986) 121.
[8] P. Haro-González, F. Lahoz, J. González-Platas, J.M. Cáceres, S. González-Pérez, D. Marreno-López, N. Capuj, I.R. Martín, J. Lumin. 128 (2008) 908.
[9] F. Auzel, C.R. Acd, Sci. Ser. I: Math. 262 (1966) 1016.
[10] Fiorenzo Vetrone, J.Christopher Boyer, John A. Capobianco, Adolfo Speghini, Marco Bettinelli, J. Phys. Chem. B 107 (2003) 1107.
[11] N.V. Kuleshov, A.A. Lagatsky, V.G. Shcherbitsky, V.P. Mikhailov1, E. Heumann, T. Jensen, A. Diening, G. Huber., Appl. Phys. B 64 (1997) 409.
[12] H. Shi-hua, L. Li-ren., Acta Phys. Sin. 38 (1989) 422.
[13] A. Brenier, G. Boulon, C. Madej, C. Pédrini., J. Lumin. 54 (1993) 271.
[14] M. Inokuti, F. Hirayama., J. Chem. Phys. 43 (1978) 1965.
[15] I.R. Martín, V.D. Rodríguez, U.R. Rodríguez-Mendoza, V. Lavín, E. Montoya, D. Jaque, J. Chem. Phys. 111 (1999) 1191.
[16] S. Bjurshagen, J. Hellström, V. Pasiskevicius, M. Cinta-Pujol, M. Aguiló, F. Díaz, Appl. Opt. 45 (2006) 4715.
[17] F. Li, Q.Y. Zhang, Y.P. Lee., J. Appl. Phys. 96 (2004) 4746.
[18] C.C. Ting, S.Y. Chen, H.Y. Le., J. Appl. Phys. 94 (2003) 2102.
[19] D.C. Yeh, W.A. Siblei, M. Suscavage, M.G. Drexhage, J. Appl. Phys. 62 (1987) 266.
[20] I.R. Martín, V.D. Rodríguez, U.R. Rodríguez-Mendoza, V. Lavín, Phys. Rev. B 57 (1998) 3396.